IOP Conf. Series: Journal of Physics: Conf. Series **843** (2017) 012014 doi:10.1088/1742-6596/843/1/012014

Analysis of multiple edge cracks in a non-homogeneous piezoelectric layer

M. Nourazar, M. Ayatollahi
Faculty of Engineering, University of Zanjan, P. O. Box 45195-313, Zanjan, Iran
Corresponding author's: mo.ayatollahy@gmail.com

Abstract. This study is concerned with the treatment of the several edge cracks in a functionally graded piezoelectric (FGP) layer under anti-plane mechanical and in-plane electrical loading. The edge crack is assumed to be either electrically impermeable or permeable. The problem is formulated by using distributed dislocation technique. The integral equations are constructed for the analysis of a FGP layer, in which the unknown variables are dislocation densities. By use of the dislocation densities, the field intensity factors are calculated. Numerical examples are provided to show the effect of the location and orientations of edge crack upon the stress intensity factors.

1. Introduction

Piezoelectric materials generate an electric field when subjected to strain fields and undergo deformation when an electric field is applied. This inherent electromechanical coupling is widely used in electronic industry. The technical applications include wave guides, sensors, phase invertors, transducers. Studies on the properties of piezoelectric composites have been carried out by numerous investigators. In particular, there is a growing interest among researchers in solving fracture mechanics problems. Because piezoelectric composite materials are very brittle and cracked piezoelectric composite materials usually contain multiple cracks, the interaction between cracks may significantly affect their fracture behavior.

There has been significant progress in the study of electroelastic fields disturbed by cracks in piezoelectric materials recently. The problem of a finite crack in a strip of FGPM was analyzed by Li and Weng [1]. Wang [2] studied a mode-III crack in FGPMs. A FGPM strip with eccentric crack under anti-plane shear was analyzed by Shin and Kim [3]. Hu et al. [4] and Yong and Zhou [5] studied both the impermeable and permeable cracks in a FGPM layer bonded to two dissimilar homogeneous piezoelectric half spaces. Zhou and Wang [6] solved an anti-plane shear crack in FGPMs using non-local theory. Jiang [7] investigated the fracture behavior of FGPMs with dielectric cracks. Zhou and Chen [8] studied the interaction of two parallel mode-I limited-permeable cracks in a FGPM. Interaction between an electrically permeable crack and the imperfect interface in FGPM was solved by Li and Lee [9]. Yan and Jiang [10] investigated the parallel cracks in FGPMs.

In the present study, the interactions of multiple edge cracks in a FGP strip investigated using the distributed dislocation technique. The Fourier transform was employed to reduce boundary value problem to the integral equations. Numerical results are provided to show the effects of the length and distance of cracks on the field intensity factors.

2. Formulation of the problem

Consider FGP layer with the poling axis z occupies the region, and is thick enough in the z-direction to allow a state of anti-plane shear. The FGP layer containing a Volterra-type screw dislocation with the line of dislocation parallel to the edges of the layer is analyzed. The piezoelectric boundary value problem is simplified considerably if we consider only the out-of-plane mechanical and the in-plane electric fields such that:

$$u = 0, v = 0, w = w(x, y)$$

Content from this work may be used under the terms of the Creative Commons Attribution 3.0 licence. Any further distribution of this work must maintain attribution to the author(s) and the title of the work, journal citation and DOI.
Published under licence by IOP Publishing Ltd

$$E_x = E_x(x,y),\ E_y = E_y(x,y),\ E_z = 0. \tag{1}$$

In this case, the constitutive equations for the piezoelectric material can be expressed as

$$\begin{aligned}
\sigma_{xz} &= c_{44}(y)\frac{\partial w}{\partial x} + e_{15}(y)\frac{\partial \varphi}{\partial x} \\
\sigma_{yz} &= c_{44}(y)\frac{\partial w}{\partial y} + e_{15}(y)\frac{\partial \varphi}{\partial y} \\
D_x &= e_{15}(y)\frac{\partial w}{\partial x} - \varepsilon_{11}(y)\frac{\partial \varphi}{\partial x} \\
D_y &= e_{15}(y)\frac{\partial w}{\partial y} - \varepsilon_{11}(y)\frac{\partial \varphi}{\partial y}
\end{aligned} \tag{2}$$

where $c_{44}(y)$ is the elastic stiffness measured in a constant electric field, $e_{15}(y)$ is the piezoelectric constant and $\varepsilon_{11}(y)$ is the dielectric measured at a constant strain. The elastic displacement and electric potential must satisfy the governing equations as follows:

$$\begin{aligned}
c_{44}(y)\nabla^2 w + e_{15}(y)\nabla^2\varphi + \frac{\partial c_{44}(y)}{\partial y}\frac{\partial w}{\partial y} + \frac{\partial e_{15}(y)}{\partial y}\frac{\partial \varphi}{\partial y} = 0 \\
e_{15}(y)\nabla^2 w - \varepsilon_{11}(y)\nabla^2\varphi + \frac{\partial e_{15}(y)}{\partial y}\frac{\partial w}{\partial y} - \frac{\partial \varepsilon_{11}(y)}{\partial y}\frac{\partial \varphi}{\partial y} = 0
\end{aligned} \tag{3}$$

The material properties of the FGP layer are adopted as follows:

$$\begin{aligned}
c_{44}(y) &= c_{440}e^{2\lambda y}, \quad e_{15}(y) = e_{150}e^{2\lambda y} \\
\varepsilon_{11}(y) &= \varepsilon_{110}e^{2\lambda y}, \quad \rho(y) = \rho_0 e^{2\lambda y}
\end{aligned} \tag{4}$$

where λ is the non-homogeneous material constant and $[c_{440}, e_{150}, \varepsilon_{110}, \rho_0]$ are values at the plane $y = 0$. The above assumption is unrealistic for all the material properties, however it would allow us to shed some light on the influence of the material gradient upon the stress intensity factors. Under the above consideration, the governing equations can be simplified to the following forms:

$$\begin{aligned}
c_{440}\nabla^2 w + e_{150}\nabla^2\varphi + 2\lambda c_{440}\frac{\partial w}{\partial y} + 2\lambda e_{150}\frac{\partial \varphi}{\partial y} = 0 \\
e_{150}\nabla^2 w - \varepsilon_{110}\nabla^2\varphi + 2\lambda e_{150}\frac{\partial w}{\partial y} - 2\lambda\varepsilon_{110}\frac{\partial \varphi}{\partial y} = 0.
\end{aligned} \tag{5}$$

With the use of Bleustein function

$$\psi(x,y) = \varphi - \alpha w(x,y) \tag{6}$$

In which $\alpha = e_{150}/\varepsilon_{110}$, Eqs. (5) can be written as follows:

$$\begin{aligned}
\nabla^2 w + 2\lambda\frac{\partial w}{\partial y} = 0, \\
\nabla^2\psi + 2\lambda\frac{\partial \psi}{\partial y} = 0.
\end{aligned} \tag{7}$$

where $\tilde{c}_{44} = c_{440} + (e_{150})^2/\varepsilon_{110}$ is the piezoelectric stiffened elastic constant. The constitutive equation (2) can be written as follows

$$\sigma_{xz}(\mathrm{x},\mathrm{y}) = [(c_{440} + \alpha e_{150})\frac{\partial w}{\partial x} + e_{150}\frac{\partial \psi}{\partial x}]\exp(2\lambda y)$$
$$\sigma_{yz}(\mathrm{x},\mathrm{y}) = [(c_{440} + \alpha e_{150})\frac{\partial w}{\partial y} + e_{150}\frac{\partial \psi}{\partial y}]\exp(2\lambda y)$$
$$D_x(\mathrm{x},\mathrm{y}) = -\varepsilon_{110}\exp(2\lambda y)\frac{\partial \psi}{\partial x}$$
$$D_y(\mathrm{x},\mathrm{y}) = -\varepsilon_{110}\exp(2\lambda y)\frac{\partial \psi}{\partial y} \tag{8}$$

From the physical viewpoint, two electrical crack boundary conditions have been commonly used to describing the fracture behavior in the piezoelectric materials, permeable and impermeable ones. Of these extreme cases for the crack boundary conditions where permittivity of these cracks are assumed to be infinite and zero for a slit-like crack,respectively. For impermeable case, by the using equation (6), the following conditions for screw dislocation are considered,

$$\sigma_{yz}(x,0) = 0, \quad \sigma_{yz}(x,h) = 0, \quad \sigma_{yz}(x,\zeta^-) = \sigma_{yz}(x,\zeta^+),$$
$$D_y(x,0) = 0, \quad D_y(x,h) = 0, \quad D_y(x,\zeta^-) = D_y(x,\zeta^+),$$
$$w(x,\zeta^-) - w(x,\zeta^+) = b_{mz}H(x-\eta),$$
$$\psi(x,\zeta^-) - \psi(x,\zeta^+) = (b_p - \alpha b_{mz})H(x-\eta), \lim_{|x|\to\infty} w = 0, \lim_{|x|\to\infty} \psi = 0, \tag{9}$$

where in Eq. (9) b_{mz} and b_p designate dislocation Burgers vectors. Although the jump in the electric potential is not a type of dislocation, it is referred here as electric dislocation for convenience. To solve the problem stated above, it is convenient to employ Fourier transforms to Eqs. (7) and (9). Let the solutions of Eqs. (7) be given by:

$$w(x,y) = \frac{b_{mz}e^{-\lambda(y-\xi)}}{4\pi}\int_{-\infty}^{+\infty}\frac{\sinh[\beta(\xi-h)]}{\beta\sinh(\beta h)}(\pi\delta(\omega) - i/\omega)\left(\beta\cosh\beta y + \lambda\sinh\beta y\right)e^{i\omega x}d\omega$$
$$0 < y < \xi$$
$$w(x,y) = \frac{b_{mz}e^{-\lambda(y-\xi)}}{4\pi}\int_{-\infty}^{+\infty}\frac{\sinh(\beta\xi)}{\beta\sinh(\beta h)}(\pi\delta(\omega) - i/\omega)(\beta\cosh[\beta(y-h)] + \lambda\sinh[\beta(y-h)])e^{i\omega(x-\eta)}d\omega$$
$$\xi < y < h$$
$$\psi(x,y) = \frac{(b_p - \alpha b_{mz})e^{-\lambda(y-\xi)}}{4\pi}\int_{-\infty}^{+\infty}\frac{\sinh[\beta(\xi-h)]}{\beta\sinh(\beta h)}(\pi\delta(\omega) - i/\omega)\left(\beta\cosh\beta y + \lambda\sinh\beta y\right)e^{i\omega(x-\eta)}d\omega$$
$$0 < y < \xi$$
$$\psi(x,y) = \frac{(b_p - \alpha b_{mz})e^{-\lambda(y-\xi)}}{4\pi}$$
$$\times\int_{-\infty}^{+\infty}\frac{\sinh(\beta\xi)}{\beta\sinh(\beta h)}(\pi\delta(\omega) - i/\omega)[\beta\cosh(\beta(y-h)) + \lambda\sinh(\beta(y-h))]e^{i\omega(x-\eta)}d\omega$$
$$\xi < y < h \tag{10}$$

where $\beta = \sqrt{\lambda^2 + \omega^2}$. In this case, with the aid of constitutive equations the stress and electric displacement components are as follows:

$$\sigma_{zx}(x,y) = -\frac{e^{\lambda(\xi+y)}}{2\pi}(c_{440}b_{mz} + e_{150}b_p) \times \int_0^\infty \frac{\sinh[\beta(h-\xi)]}{\beta\sinh(\beta h)}\left(\beta\cosh\beta y + \lambda\sinh\beta y\right)\cos(\omega(x-\eta))d\omega, \quad 0 < y < \xi$$

$$\sigma_{zx}(x,y) = \frac{e^{\lambda(\xi+y)}}{2\pi}(c_{440}b_{mz} + e_{150}b_p) \times \int_0^\infty \frac{\sinh(\beta\xi)}{\beta\sinh(\beta h)}\left(\beta\cosh[\beta(y-h)] + \lambda\sinh[\beta(y-h)]\right)\cos(\omega(x-\eta))d\omega, \quad \xi < y < h$$

$$\sigma_{zy}(x,y) = (c_{440} + \alpha e_{150})\frac{e^{\lambda(\xi+y)}b_{mz}}{\pi}\int_0^\infty \frac{\omega\sinh[\beta(\xi-h)]}{\beta\sinh(\beta h)}\sinh(\beta y)\sin(\omega(x-\eta))d\omega + \frac{e_{150}(b_p - \alpha b_{mz})e^{\lambda(\xi+y)}}{\pi}\int_0^\infty \frac{\omega\sinh[\beta(\xi-h)]}{\beta\sinh(\beta h)}\sinh(\beta y)\sin(\omega(x-\eta))d\omega \qquad 0 < y < \xi$$

$$\sigma_{zy}(x,y) = (c_{440} + \alpha e_{150})\frac{e^{\lambda(\xi+y)}b_{mz}}{\pi}\int_0^\infty \frac{\omega\sinh(\beta\xi)}{\beta\sinh(\beta h)}\sinh(\beta(y-h))\sin(\omega(x-\eta))d\omega + \frac{e_{150}(b_p - \alpha b_{mz})e^{\lambda(\xi+y)}}{\pi}\int_0^\infty \frac{\omega\sinh(\beta\xi)}{\beta\sinh(\beta h)}\sinh(\beta(y-h))\sin(\omega(x-\eta))d\omega \qquad \xi < y < h$$

$$D_x(x,y) = \frac{\varepsilon_{110}(b_p - \alpha b_{mz})e^{\lambda(\xi+y)}}{2\pi}\int_0^\infty \frac{\sinh[\beta(h-\xi)]}{\beta\sinh(\beta h)}\left(\beta\cosh\beta y + \lambda\sinh\beta y\right)\cos(\omega(x-\eta))d\omega, \qquad 0 < y < \xi$$

$$D_x(x,y) = -\frac{\varepsilon_{110}(b_p - \alpha b_{mz})e^{\lambda(\xi+y)}}{2\pi} \times \int_0^\infty \frac{\sinh(\beta\xi)}{\beta\sinh(\beta h)}\left(\beta\cosh[\beta(y-h)] + \lambda\sinh[\beta(y-h)]\right)\cos(\omega(x-\eta))d\omega, \quad \xi < y < h$$

$$D_y(x,y) = -\frac{\varepsilon_{110}(b_p - \alpha b_{mz})e^{\lambda(\xi+y)}}{\pi}\int_0^\infty \frac{\omega\sinh(\beta(\xi-h))}{\beta\sinh(\beta h)}\sinh(\beta y)\sin(\omega(x-\eta))d\omega \qquad 0 < y < \xi$$

$$D_y(x,y) = -\frac{\varepsilon_{110}(b_p - \alpha b_{mz})e^{\lambda(\xi+y)}}{\pi}\int_0^\infty \frac{\omega\sinh(\beta\xi)}{\beta\sinh(\beta h)}\sinh(\beta(y-h))\sin(\omega(x-\eta))d\omega \qquad \xi < y < h \tag{11}$$

It may be seen that the integrals in (11) are bounded at $\omega = 0$. If we further observe that the integrands in (11) are continuous functions of ω, it is then clear that any singularity the kernels must be due to the asymptotic behavior of the integrands as $|\omega|$ approaches infinity. By adding and subtracting the asymptotic expressions of the integrands, we find:

$$\sigma_{zx}(x,y)=-\frac{e^{\lambda(\xi+y)}(c_{440}b_{mz}+e_{150}b_p)}{2\pi}\left\{\frac{y-\xi}{(x-\eta)^2+(y-\xi)^2}\right.$$
$$\left.-\int_0^\infty[\frac{(1-\mathrm{e}^{-2\beta(\mathrm{h}-\xi)})\left(\beta(1+\mathrm{e}^{-2\beta y})+\lambda(1-\mathrm{e}^{-2\beta y})\right)}{\beta(1-\mathrm{e}^{-2\beta h})}-1]\mathrm{e}^{\omega(y-\xi)}\cos(\omega(x-\eta))d\omega\right\},\qquad 0<y<\xi$$

$$\sigma_{zx}(x,y)=-\frac{e^{\lambda(\xi+y)}(c_{440}b_{mz}+e_{150}b_p)}{2\pi}\left\{\frac{y-\xi}{(x-\eta)^2+(y-\xi)^2}\right.$$
$$\left.+\int_0^\infty[\frac{(1-\mathrm{e}^{-2\beta\xi})\left(\beta(1+\mathrm{e}^{2\beta(y-h)})+\lambda(\mathrm{e}^{2\beta(y-h)}-1)\right)}{\beta(1-\mathrm{e}^{-2\beta h})}-1]\mathrm{e}^{-\omega(\mathrm{y}-\xi)}\cos(\omega(x-\eta))d\omega\right\},\qquad \xi<y<h$$

$$\sigma_{zy}(x,y)=\frac{(c_{440}b_{mz}+e_{150}b_p)e^{\lambda(\xi+y)}}{2\pi}\left\{\frac{x-\eta}{(x-\eta)^2+(y-\xi)^2}\right.$$
$$\left.+\int_0^\infty[\frac{\omega(\mathrm{e}^{2\beta(\xi-h)}-1)(1-\mathrm{e}^{-2\beta y})}{\beta(1-\mathrm{e}^{-2\beta h})}-1]\mathrm{e}^{\omega(y-\xi)}\sin(\omega(x-\eta))d\omega\right\}\qquad 0<y<\xi$$

$$\sigma_{zy}(x,y)=\frac{(c_{440}b_{mz}+e_{150}b_p)e^{\lambda(\xi+y)}}{2\pi}\left\{\frac{x-\eta}{(x-\eta)^2+(y-\xi)^2}\right.$$
$$\left.-\int_0^\infty[\frac{\omega(1-\mathrm{e}^{-2\beta\xi})(\mathrm{e}^{2\beta(y-h)}-1)}{\beta(1-\mathrm{e}^{-2\beta h})}+1]\mathrm{e}^{-\omega(\mathrm{y}-\xi)}\sin(\omega(x-\eta))d\omega\right\}\qquad \xi<y<h$$

$$D_y(x,y)=\frac{\varepsilon_{110}(\alpha b_{mz}-b_p)e^{\lambda(\xi+y)}}{2\pi}\left\{\frac{x-\eta}{(x-\eta)^2+(y-\xi)^2}\right.$$
$$\left.+\int_0^\infty[\frac{\omega(\mathrm{e}^{2\beta(\xi-h)}-1)(1-\mathrm{e}^{-2\beta y})}{\beta(1-\mathrm{e}^{-2\beta h})}-1]\mathrm{e}^{\omega(y-\xi)}\sin(\omega(x-\eta))d\omega\right\}\qquad 0<y<\xi$$

$$D_y(x,y)=\frac{\varepsilon_{110}(\alpha b_{mz}-b_p)e^{\lambda(\xi+y)}}{2\pi}\left\{\frac{x-\eta}{(x-\eta)^2+(y-\xi)^2}\right.$$
$$\left.-\int_0^\infty[\frac{\omega(1-\mathrm{e}^{-2\beta\xi})(\mathrm{e}^{2\beta(y-h)}-1)}{\beta(1-\mathrm{e}^{-2\beta h})}+1]\mathrm{e}^{-\omega(\mathrm{y}-\xi)}\sin(\omega(x-\eta))d\omega\right\}\qquad \xi<y<h$$

$$D_x(x,y)=\frac{(e_{150}b_{mz}-\varepsilon_{110}b_p)e^{\lambda(\xi+y)}}{2\pi}\left\{-\frac{y-\xi}{(x-\eta)^2+(y-\xi)^2}\right.$$
$$\left.+\int_0^\infty[\frac{(1-\mathrm{e}^{-2\beta(\mathrm{h}-\xi)})\left(\beta(1+\mathrm{e}^{-2\beta y})+\lambda(1-\mathrm{e}^{-2\beta y})\right)}{\beta(1-\mathrm{e}^{-2\beta h})}-1]\mathrm{e}^{\omega(y-\xi)}\cos(\omega(x-\eta))d\omega\right\},\qquad 0<y<\xi$$

$$D_x(x,y) = -\frac{(e_{150}b_{mz} - \varepsilon_{110}b_p)e^{\lambda(\xi+y)}}{2\pi}\left\{\frac{y-\xi}{(x-\eta)^2+(y-\xi)^2}\right.$$
$$\left.+\int_0^\infty [\frac{(1-\mathrm{e}^{-2\beta\xi})\left(\beta(1+\mathrm{e}^{2\beta(y-h)})+\lambda(\mathrm{e}^{2\beta(y-h)}-1)\right)}{\beta(1-\mathrm{e}^{-2\beta h})}-1]\mathrm{e}^{-\omega(y-\xi)}\cos(\omega(x-\eta))d\omega\right\}, \qquad \xi < y < h \tag{12}$$

We may observe that stress components exhibit the familiar Cauchy-type singularity at dislocation location.

The dislocation solutions accomplished in the preceding section may be employed to analyze FGP layer containing several edge cracks with any arrangement. A crack configuration with respect to coordinate system *x*, *y* may be described in parametric form as:

$$x_i = x_i(s)$$
$$y_i = y_i(s) \qquad i = 1,2,...,N \qquad -1 \le s \le 1 \tag{13}$$

Next, covering the crack surfaces by dislocations, the principle of superposition is invoked to obtain the tractions on a given crack surface. The anti-plane traction and electric potential components on the face of the *i*th crack due to the presence of distribution of the above-mention dislocations on all *N* cracks yields.

$$\sigma_{yz}(x_i(s), y_i(s)) = \sum_{j=1}^{N}\int_{-1}^{1}[K_{ij}^{11}(s,t)B_{mzj}(t) + K_{ij}^{12}(s,t)B_{pj}(t)]l_j\,dt$$
$$D_y(x_i(s), y_i(s)) = \sum_{j=1}^{N}\int_{-1}^{1}[K_{ij}^{21}(s,t)B_{mzj}(t) + K_{ij}^{22}(s,t)B_{pj}(t)]l_j\,dt \tag{14}$$

By virtue of Bueckner's principle (see, e.g., Hills et al., 1996), the left hand side of Eqs. (14) are stress components and the electric displacement at the presumed location of the cracks with negative sign, which implies impermeable crack boundary conditions. From the definition of density function, the equation for the crack opening displacement and electric potential across *j*th crack become

$$w_j^-(s) - w_j^+(s) = \int_{-1}^{s} l_j B_{mj}(t)dt$$
$$\phi_j^-(s) - \phi_j^+(s) = \int_{-1}^{s} l_j B_{pj}(t)dt \tag{15}$$

For the edge cracks, taking the embedded crack tip at $t = -1$, the dislocation densities may be expressed as:

$$B_{kj}(t) = g_{kj}(t)\sqrt{1-t/1+t}, \quad -1 \le t \le 1, \quad k \in \{m, p\} \tag{16}$$

The parameters $g_{kj}(t)$ are obtained by solving the system of equations (14, 16). The stress and electric intensity factors for edge crack take the forms

$$(K_{III}^m)_{Li} = c_{44}(y_{Li})\left[[(x_i'(-1)]^2 + [y_i'(-1)]^2\right]^{\frac{1}{4}} g_{mi}(-1) + e_{15}(y_{Li})\left[[(x_i'(-1)]^2 + [y_i'(-1)]^2\right]^{\frac{1}{4}} g_{pi}(-1)$$
$$(K_{III}^D)_{Li} = e_{15}(y_{Li})\left[[(x_i'(-1)]^2 + [y_i'(-1)]^2\right]^{\frac{1}{4}} g_{mi}(-1) - \varepsilon_{11}(y_{Li})\left[[(x_i'(-1)]^2 + [y_i'(-1)]^2\right]^{\frac{1}{4}} g_{pi}(-1) \tag{17}$$

For brevity, the details of the derivation of fields intensity factors are not given here.

3. Numerical results and discussion

The analysis developed in the preceding section allows the consideration a FGP layer with any number of cracks with different shape and orientations. In the computational procedure, we consider the PZT-4 piezoelectric ceramic of which material properties are given as follows:

$$c_{44} = 2.56\times10^{10}\,\frac{N}{m^2}, e_{15} = 12.7\,\frac{C}{m^2}, \varepsilon_{11} = 64.6\times10^{-10}\,\frac{C}{Vm}, \rho_0 = 7.5\times10^{3}\,\frac{kg}{m^3}$$

where N is the force in Newton, C is the charge in Coulomb and V is the electric potential in Volt. The stress intensity factor is normalized by $K_0 = \tau_0\sqrt{L}$ and electromechanical coupling factor that we used is defined by $ecf = D_0 e_{15}/\tau_0\varepsilon_{11}$.

The first example is considered the problem of a functionally graded piezoelectric layer weakened by an edge crack. The applied loads are constant anti-plane mechanical ($\sigma_{xz}=\sigma_0$) and in-plane electrical loading with magnetiude (D_0), while $D_0 e_{15}/\tau_0\varepsilon_{11} = 1.0$. The plot of the normalized stress intensity factor versus crack length for different values of the non-homogeneous parameter (λh=0,1) is shown in Fig (1). Increasing the non-homogeneous parameter results in lower stress intensity factor. Fig. (1) also shows that the stress intensity factor increases with an increase in crack length for two different electric boundary conditions.

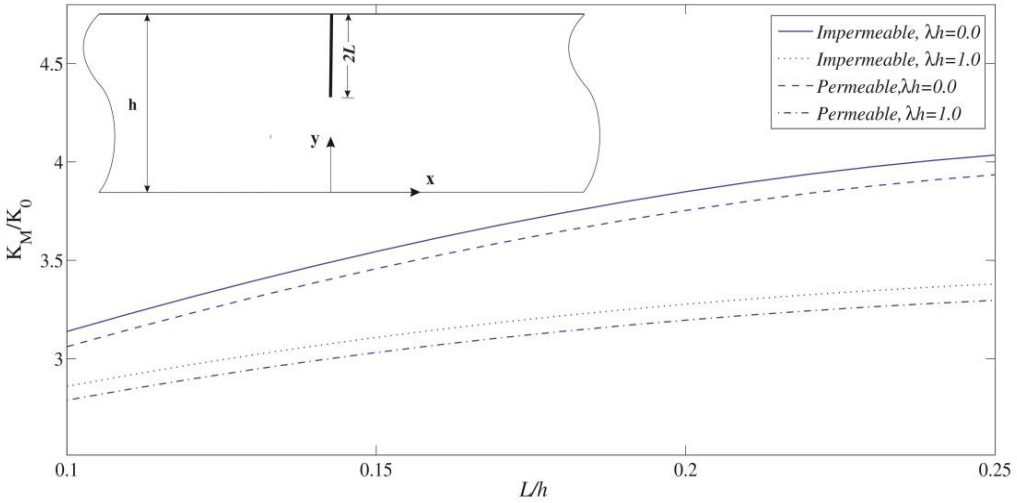

Fig. 1. Variation of stress intensity factors for an edge crack versus L/h.

Fig. (2) shows the normalized stress intensity factor, K_M / K_0 as function of the non-homogeneous parameter λL and for different crack orientations. As it may be observed, the stress intensity factor decreases rapidly as λL increases. The similar trend may be noticed for the two different electric boundary conditions.

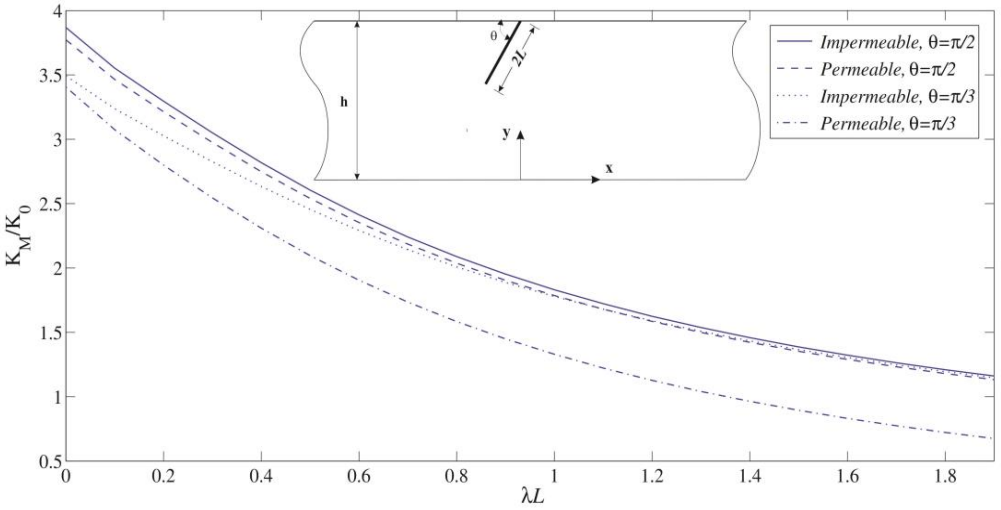

Fig. 2. Variation of stress intensity factors for an edge crack versus λL.

The effect of crack orientation on the stress intensity factor is examined by considering an edge crack with constant length (Fig. 3). As the crack angle increases, the stress intensity factors increase. The maximum stress intensity factor for the crack tips occur when the crack surface traction is maximum. The trend of variation of stress intensity factor remains the same by changing the FGM constant.

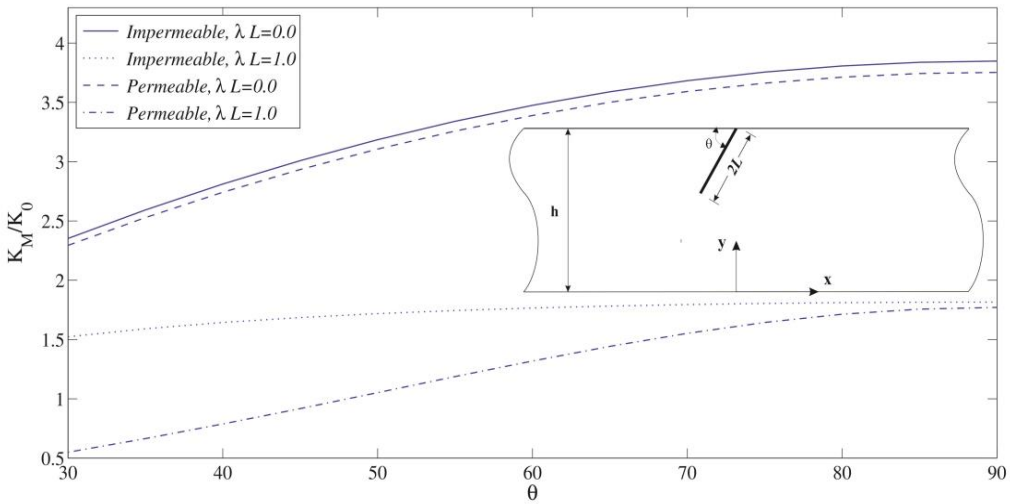

Fig. 3. Variation of stress intensity factors for a rotating edge crack.

In the next example, the FGP layer containing two parallel cracks with equal length is considered. The variations of K_M / K_0 with crack length is depicted in Fig(4) for three different crack distances. When the distance between the crack tips is minimum obviously experiences higher stress intensity factors.

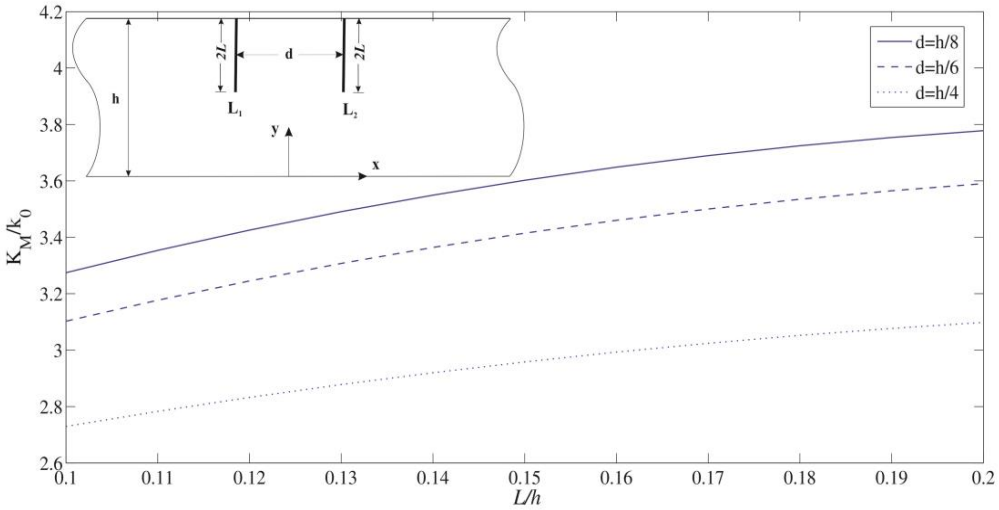

Fig. 4. Variation of stress intensity factors of two parallel edge crack.

In the last example, the interaction between two equal-length edge cracks is examined. The dimensionless stress intensity factors versus the crack orientation is shown in Fig. (5). As it was expected, the variation of stress intensity factor of rotating crack tip L_2 is more pronounced than that of the tip L_1.

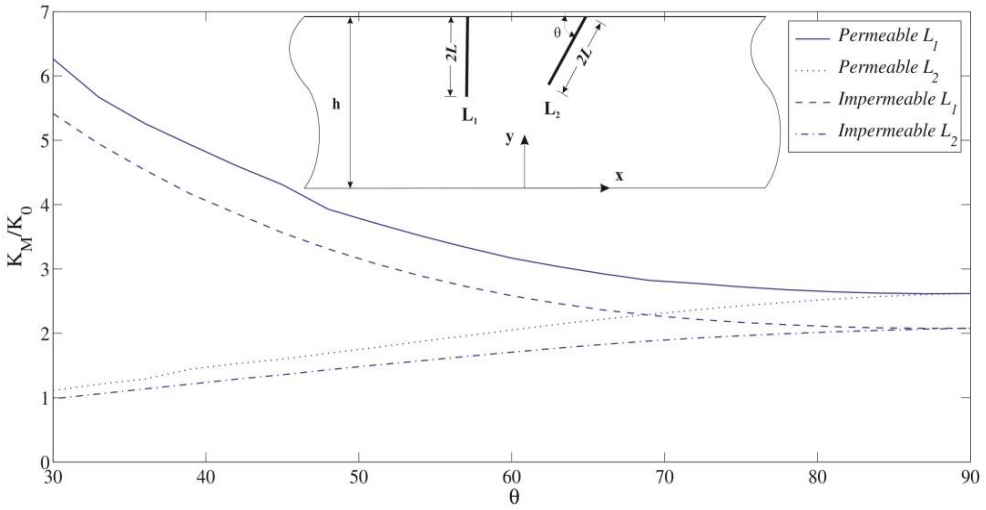

Fig. 5. Variation of stress intensity factors of two intracting edge crack.

4. Conclusions

The present work deals with the behavior of a FGP layer containing multiple edge cracks subjected to electro-mechanical loads. The dislocation solution is utilized to perform integral equations for FGP layer with multiple edge cracks. These equations are of Cauchy singular type solvable by numerical methods to obtain dislocation density on the crack surfaces. Numerical calculations are carried out to study the effect of the geometry of the several edges cracks and the material properties on the resulting stress intensity factor.

References

[1] Li C and Weng GJ, 2002a Anti-plane crack problem in functionally gradedpiezoelectric materials, ASME J. Appl. Mech. **69** 481–488
[2] Wang BL 2003 A mode-III crack in functionally graded piezoelectric materials, Mech. Res. Commun. **30** 151–159
[3] Shin JW and Kim TU 2003. Functionally graded piezoelectric strip with eccentriccrack under anti-plane shear, J. Mech. Sci. Technol. **17** 854–859
[4] Hu KQ, Zhong Z and Jin B 2005 Anti-plane shear cracking functionally gradientpiezoelectric layer bonded to dissimilar half spaces, Int. J. Mech. Sci. **47** 82–93
[5] Yong HD and Zhou YH 2007 A mode-III crack in a functionally graded piezoelectricstrip bonded to two dissimilar piezoelectric half-planes, Compos. Struct. **79** 404–410
[6] Zhou ZG and Wang B 2006 Non-local theory solution for an anti-plane shearpermeable crack in functionally graded piezoelectric materials, Appl. Compos. Mater. **13** 345–367
[7] Jiang LY 2008 The fracture behavior of functionally graded piezoelectric materialswith dielectric cracks, Int. J. Fract. **149** 87–104
[8] Zhou Z and Chen ZT 2008 The interaction of two parallel mode-I limitedpermeable cracks in a functionally graded piezoelectric material, Euro. J. Mech. A Solids **27** 824–846
[9] Li YD and Lee KY 2009a Interaction between an electrically permeable crack andthe imperfection interface in a functionally graded piezoelectric sensor, Int. J. Eng. Sci. **47** 363–371
[10] Yan Z and Jiang LY 2010 Interaction of parallel dielectric cracks in functionallygraded piezoelectric materials, Acta Mech. **211** 251–269
[11] Hills DA, Kelly PA, Dai DN and Korsunsky AM 1996. Solution of Crack Problems: The Distributed Dislocation Technique, Kluwer: Academic Publishers